Simplified expansions for radiation from a baffled circular piston

T. Douglas Mast
Department of Biomedical Engineering, University of Cincinnati, Cincinnati, Ohio 45267-0586

Feng Yu[a)]
Department of Aerospace Engineering and Engineering Mechanics, University of Cincinnati, Cincinnati, Ohio 45221-0070

(Received 31 May 2005; revised 1 September 2005; accepted 5 September 2005)

Computation of acoustic radiation from a baffled circular piston continues be an active area of investigation, both as a canonical problem and because of numerous practical applications. For time-harmonic radiation, exact series expansions are an attractive approach because they do not require numerical integration or limiting approximations. Here, series expansions due to Hasegawa, Inoue, and Matsuzawa [J. Acoust. Soc. Am. **74**, 1044–1047 (1983); **75**, 1048–1051 (1984)] are shown to reduce to simpler expressions suitable for numerical computations of piston fields in lossless and attenuative fluid media. For the region $r \geqslant a$, where a is the piston radius and r is the distance from the piston center, an exact solution is given by an series of spherical Hankel functions and Legendre polynomials with explicit, closed-form, position-independent coefficients. For the paraxial region $w \leqslant a$, where w is the distance from the piston axis, a second exact series expansion is valid for all axial distances z and reduces to the known analytic solution for $w=0$. These two expansions allow the radiated field to be computed at any point, with rapid convergence except for points near the circle bounding the piston. Example numerical results illustrate application of this method to ultrasonic sources. © *2005 Acoustical Society of America.* [DOI: 10.1121/1.2108997]

PACS number(s): 43.20.Rz, 43.20.El [JJM] Pages: 3457–3464

I. INTRODUCTION

Acoustic radiation from a circular piston is a canonical acoustics problem investigated by Rayleigh and many subsequent researchers. In this problem, a circular piston with radius a, within an infinite rigid baffle, vibrates uniformly at a radial frequency ω with a normal velocity $v_0 e^{-i\omega t}$ into a homogeneous fluid medium with speed of sound c and density ρ. The resulting radiated pressure is given by the Rayleigh integral[1]

$$p(\mathbf{r},t) = -\frac{ik}{2\pi} p_0 \int \frac{e^{ikR}}{R} dS e^{-i\omega t}, \tag{1}$$

where $p_0 = \rho c v_0$, $R = |\mathbf{r} - \mathbf{r}_s|$ is the distance from a field point $\mathbf{r}$ to a point on the piston surface $\mathbf{r}_s$, k is the wave number ω/c (which is complex in the case of a sound-absorbing medium), and S covers all points on the piston surface, $r_s \leqslant a$.

The Rayleigh integral is not directly solvable in a simple form, except for certain special cases, including the on-axis field and the asymptotic far field.[2] Piston fields have often been computed using numerical integration, including methods that transform the Rayleigh integral into single line integrals[3–6] and methods involving numerical integration of the space- and time-dependent piston impulse response.[7–9] Because of the problem's practical importance in ultrasonics and other areas of acoustics, the efficient computation of such numerical integrals,[10–12] as well as approximations to the piston field,[13–17] remain active areas of research.

An alternate approach to exact computation of piston fields involves expansion of the field in series of orthogonal functions. Series solutions have advantages including exactness, easily analyzed convergence properties, and amenability to analysis. Series of this form were derived by Backhaus[18] and Stenzel,[19] who presented equivalent expansions valid for the region $r \geqslant a$, where r is the distance from the piston center. These expansions are slow to converge for $r \approx a$, while an additional solution by Stenzel for the region $r \leqslant a$ is slow to converge over the entire region $r \leqslant a$.[19,20] More recently, Wittmann and Yaghjian[20] presented an alternate derivation of the Backhaus-Stenzel series for $r \geqslant a$ and a different expansion for $r \leqslant a$, which incurs similar convergence problems for $r \approx a$. Other available series expansions include an expression in oblate spheroidal coordinates by Spence[21] that is slow to converge for large ka, an expansion derived by Carter and Williams[22,23] and improved by Elrod[24] that is invalid for $z \leqslant a$ and is slow to converge outside the paraxial region, and a slowly-converging series derived by New as a limiting case of a radially vibrating polar cap on a rigid sphere.[25]

More general series expansions were derived by Hasegawa, Inoue, and Matsuzawa.[26,27] These series contain coefficients that depend on the spatial position and on the choice of an origin for the coordinate system employed. For a given field position, choice of an appropriate origin location provides a series with favorable local convergence properties. However, simpler expressions that do not depend on spatial position or choice of origin would be desirable for numerical computation of piston radiator fields.

[a)]Present address: Cessna Aircraft Company, Wichita, Kansas 67215.

Here, simplified series, which also result from special cases of the Hasegawa, Inoue, and Matsuzawa expansions, are derived. An expansion valid for $r \geqslant a$ is equivalent to previous series solutions,[18–20] but is presented here with explicit, closed-form coefficients. A second expansion is valid for $w \leqslant \sqrt{z^2+a^2}$, where w is the distance from the piston axis, and converges within a few terms for field points near the axis. Computational examples show that these two methods provide accurate solutions for the piston field, with favorable convergence properties except near the velocity discontinuity at the piston boundary, where $z \approx 0$ and $w \approx a$.

II. THEORY

A. General expansions

For simplicity, the following derivations will set $p_0 \equiv 1$ in Eq. (1) and suppress the $e^{-i\omega t}$ time dependence. An exact series solution of the Rayleigh integral by Hasegawa *et al.* is then given for the notation of Eq. (1) as[27]

$$p(r,\theta) = \sum_{n=0}^{\infty} (-1)^n (2n+1) f_n(kr_0, kr_a) P_n(\cos\theta) j_n(kr),$$
$$f_n(kr_0, kr_a) = \int_{kr_0}^{kr_a} P_n\left(\frac{kr_0}{\zeta}\right) h_n^{(1)}(\zeta)\zeta d\zeta. \tag{2}$$

Here, r_0 is distance from the piston center to the origin of the spherical coordinate system (r, θ, ϕ), which is placed arbitrarily along the piston's axis of symmetry $(r_0 > 0)$, $r_a = \sqrt{r_0^2 + a^2}$, j_n and $h_n^{(1)}$ are the spherical Bessel function and Hankel function of the first kind, and P_n is the Legendre polynomial. The integral $f_n(kr_0, kr_a)$ can be evaluated for successive indices n using a recurrence relation given in Ref. 26. According to Hasegawa *et al.*, the solution of Eq. (2) is appropriate for $r \leqslant r_a$, while for $r \geqslant r_a$ an appropriate series solution is[27]

$$p(r,\theta) = \sum_{n=0}^{\infty} (-1)^n (2n+1) \mathrm{Re}[f_n(kr_0, kr_a)] P_n(\cos\theta) h_n^{(1)}(kr). \tag{3}$$

Although exact and fairly general, computations employing Eqs. (2) and (3) are complicated by the requirement to choose an origin position r_0. The solution of Eq. (2) is slow to converge for large values of kr, and the convergence properties of Eq. (3) also depend on kr, so that the useful region for each of these expansions depends on the choice of the origin r_0. Two special cases of the above solutions can reduce these difficulties; a simplified derivation encompassing these special cases follows.

B. Simplified expansions

Below, simplified series expansions for the Rayleigh integral are derived directly from a series expansion of the integrand, As a starting point, the distance R from a field point $\mathbf{r}$ to a point on the piston surface $\mathbf{r}_s$ in Eq. (1) can be written in cylindrical coordinates as

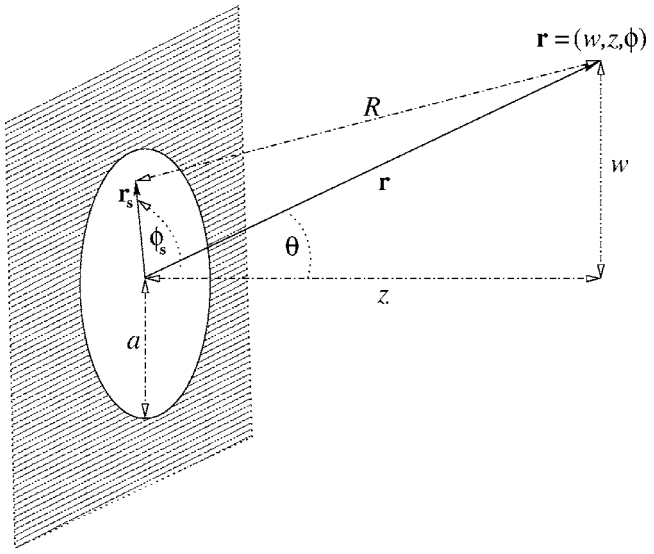

FIG. 1. Sketch of the problem geometry and notation. A piston of radius a, centered at the origin, radiates from within an infinite baffle into a semi-infinite space. The vector $\mathbf{r} = (w, z, \phi)$ is the position of a field point in cylindrical coordinates, where w is the azimuthal distance from the piston axis, z is the distance along the piston axis, and ϕ is the azimuthal angle. The vector $\mathbf{r}_s = (w_s, \phi_s)$ denotes a position on the piston surface. The angle between the z axis and the position vector $\mathbf{r}$ is denoted by θ.

$$R = \sqrt{z^2 + w^2 + w_s^2 - 2ww_s \cos\phi_s}, \tag{4}$$

where z and w are the axial and azimuthal coordinates of the field point, while w_s and ϕ_s are the azimuthal coordinate and angle of a point on the piston surface. This coordinate system, in which the origin is placed at the piston center, is sketched in Fig. 1. Without loss of generality, the azimuthal angle ϕ of the field point is taken here to be zero.

The distance defined by Eq. (4) can be rewritten as

$$R = \sqrt{r_1^2 + r_2^2 - 2r_1 r_2 \cos\phi_s \sin\beta}, \tag{5}$$

where the distances r_1 and r_2 must satisfy the relation $r_1^2 + r_2^2 = z^2 + w^2 + w_s^2$ and $\sin\beta = (ww_s)/(r_1 r_2)$ may not exceed unity.

Several different series expansions of the Rayleigh integral can then be obtained using the identity[28]

$$\frac{e^{ik\sqrt{r_1^2+r_2^2-2r_1r_2\cos\phi_s\sin\beta}}}{\sqrt{r_1^2 + r_2^2 - 2r_1 r_2 \cos\phi_s \sin\beta}} = ik \sum_{n=0}^{\infty} (2n+1) P_n(\cos\phi_s \sin\beta) j_n(kr_1) h_n^{(1)}(kr_2), \tag{6}$$

which converges for $r_1 \leqslant r_2$. Here, P_n is the Legendre polynomial, j_n is the spherical Bessel function, and h_n is the spherical Hankel function. Variants of this identity were employed in Refs. 19, 26, and 27. Inserting Eq. (6) into the Rayleigh integral (1), one obtains the series expansion

$$p(\mathbf{r}) = \frac{k^2}{2\pi}\sum_{n=0}^{\infty}(2n+1)\int_0^a\left[\int_0^{2\pi}P_n(\cos\phi_s\sin\beta)d\phi_s\right]$$
$$\times j_n(kr_1)h_n^{(1)}(kr_2)w_s dw_s$$
$$= k^2\sum_{n=0}^{\infty}(2n+1)P_n(0)\int_0^a P_n(\cos\beta)j_n(kr_1)h_n^{(1)}(kr_2)w_s dw_s$$
$$= \frac{k^2}{\sqrt{\pi}}\sum_{n=0}^{\infty}(-1)^n(4n+1)\frac{\Gamma\left(n+\frac{1}{2}\right)}{\Gamma(n+1)}$$
$$\times\int_0^a P_{2n}(\cos\beta)j_{2n}(kr_1)h_{2n}^{(1)}(kr_2)w_s dw_s. \quad (7)$$

Here, the integral over ϕ_s has been evaluated using the addition theorem for Legendre polynomials as in Refs. 19 and 26. The Legendre polynomial $P_n(0)$ has value zero for odd n, so that the series expansion of Eq. (7) contains only Legendre polynomials and spherical Bessel and Hankel functions of even order.

Given a choice of appropriate distances r_1 and r_2, construction of a series expansion solving the Rayleigh integral (1) in the region $r_1 \leqslant r_2$ requires only evaluation of the integral term in the last of Eqs. (7). One useful case is obtained by setting $r_1 = w_s$, $r_2 = \sqrt{z^2+w^2} = r$, which results in a valid series expansion if $r \geqslant a$. In this case, $\sin\beta = w/r = \sin\theta$ and Eq. (7) becomes

$$p(\mathbf{r}) = \frac{k^2}{\sqrt{\pi}}\sum_{n=0}^{\infty}(-1)^n(4n+1)\frac{\Gamma\left(n+\frac{1}{2}\right)}{\Gamma(n+1)}\left[\int_0^a j_{2n}(kw_s)w_s dw_s\right]$$
$$\times P_{2n}(\cos\theta)h_{2n}^{(1)}(kr)$$
$$= \sum_{n=0}^{\infty}(-1)^n\left(\frac{ka}{2}\right)^{(2n+2)}\frac{(4n+1)\Gamma\left(n+\frac{1}{2}\right)}{\Gamma(n+2)\Gamma\left(2n+\frac{3}{2}\right)}$$
$$\times {}_1F_2\left[n+1; n+2, 2n+\frac{3}{2}; -\left(\frac{ka}{2}\right)^2\right]$$
$$\times P_{2n}(\cos\theta)h_{2n}^{(1)}(kr). \quad (8)$$

Here, evaluation of the integral term[29] has yielded explicit coefficients in terms of the generalized hypergeometric function ${}_1F_2$. Taken as a function of $\xi \equiv ka/2$, this function is well-behaved for all orders n, with value unity for $\xi \to 0$, positive for all $\xi \geqslant 0$, and zero for $\xi \to \infty$. For large order n, this hypergeometric function approaches a Gaussian distribution

$$\lim_{n\to\infty} {}_1F_2\left[n+1; n+2, 2n+\tfrac{3}{2}; -\xi^2\right] = e^{-\xi^2/2n}, \quad (9)$$

which can be verified by expanding the hypergeometric and exponential functions from Eq. (9) in powers of ξ and evaluating the limit $n \to \infty$ term by term. The general function ${}_1F_2(a_1; b_1, b_2; -\xi^2)$ has been analyzed previously[30] and can be computed numerically with available algorithms.[31,32] Equivalently, the integral appearing in Eq. (8) can be evaluated in terms of Bessel functions and Lommel functions.[29]

The series expansion of Eq. (8) is equivalent to series derived in Refs. 18–20 for the region $r \geqslant a$, although none of these references presented explicit series coefficients. This expansion, which is valid for $r \geqslant a$ and converges smoothly except for the region $r \approx a$, can also be obtained by setting $r_0 = 0$ in Eq. (3). Numerical computations suggest that outside the region $r \approx a$, the number of terms required for convergence is of the order $N \sim ka$. Below, the solution of Eq. (8) will be referred to as an "outer" expansion, since it is valid for the region exterior to the hemisphere $r = a$.

A second useful series expansion is obtained from the choices $r_1 = w$, $r_2 = \sqrt{z^2+w_s^2}$. In this case, $\cos\beta = z/\sqrt{z^2+w_s^2}$ and Eq. (7) reduces to

$$p(\mathbf{r}) = \frac{1}{\sqrt{\pi}}\sum_{n=0}^{\infty}(-1)^n(4n+1)\frac{\Gamma\left(n+\frac{1}{2}\right)}{\Gamma(n+1)}$$
$$\times\left[\int_{kz}^{kr_a} P_{2n}\left(\frac{z}{\zeta}\right)h_{2n}^{(1)}(\zeta)\zeta d\zeta\right]j_{2n}(kw)$$
$$= \frac{1}{\sqrt{\pi}}\sum_{n=0}^{\infty}(-1)^n(4n+1)\frac{\Gamma\left(n+\frac{1}{2}\right)}{\Gamma(n+1)}f_{2n}(kz, kr_a)j_{2n}(kw), \quad (10)$$

where f_{2n} is the integral function from Eq. (2), which can be evaluated using the recurrence relation[26]

$$f_0 = e^{ikz} - e^{ikr_a},$$
$$f_{2n} = -f_{2n-2} - kr_a\left[P_{2n}\left(\frac{z}{r_a}\right) - P_{2n-2}\left(\frac{z}{r_a}\right)\right]h_{2n-1}^{(1)}(kr_a), \quad (11)$$

where $r_a = \sqrt{z^2+a^2}$. This solution corresponds to the special case $r_0 = z$ in Eq. (2). The series converges for the region $w \leqslant \sqrt{z^2+a^2}$, with fastest convergence near the piston axis $w = 0$ and slowest convergence for $w \approx \sqrt{z^2+a^2}$. Numerical experience suggests that, within the region of validity for this expansion, $N \sim kw$ terms are required for convergence at an azimuthal distance w. Because the solution of Eq. (10) converges fastest within the cylinder defined by $w \leqslant a$, this series will be referred to below as a paraxial expansion.

Notable is that the terms f_{2n} in Eq. (10) depend spatially only on the axial coordinate z. Thus, computations of the piston field at multiple spatial points (e.g., on a rectangular grid in the axial and azimuthal directions) can be performed more efficiently by computing these terms only once for each axial distance required.

Compared to the previous series expansions cited above, the expansion of Eq. (10) particularly simplifies computation of pressure fields near the piston axis. On the axis ($w = 0$), only the leading term from Eq. (10) is nonzero and the solution reduces identically to the known exact solution[2]

$$p(0,z) = e^{ikz} - e^{ikr_a} = -2ie^{ik(z+r_a)/2}\sin\left(\frac{kr_a - kz}{2}\right), \quad (12)$$

where, as above, $r_a = \sqrt{z^2+a^2}$.

Similarly, for points close to the piston axis, the paraxial expansion of Eq. (10) converges within a few terms, since each term of Eq. (10) is of order $(kw)^{2n}$. Thus, for example,

an expression valid to fourth order in the normalized azimuthal coordinate kw can be obtained from Taylor series for the first three terms of the paraxial expansion (10). The result is

$$p(w,z) = e^{ikz} - e^{ikr_a}\left[1 - \frac{a^2(kr_a+i)}{4kr_a^3}(kw)^2 + \psi(k,a,r_a)(kw)^4\right] + O[(kw)^6], \tag{13}$$

where the fourth-order term ψ is given by

$$\psi(k,a,r_a) = \frac{a^4}{64k^3r_a^7}\left\{\left[12\left(\frac{r_a}{a}\right)^2 - 15\right](kr_a+i) - i\left[4\left(\frac{r_a}{a}\right)^2 - 6\right](kr_a)^2 + (kr_a)^3\right\}. \tag{14}$$

The truncated series of Eq. (13) is accurate for points near the piston axis, relative to the acoustic wavelength. For $kw \ll 1$, this expression is more accurate than the approximate paraxial expression derived by Schoch,[2,4] and agrees to second order in kw with an improved approximation derived in Ref. 13. The fourth-order correction of Eq. (14) provides greater accuracy for small kw than either of these previous approximations.

The pressure field given by the paraxial expansion of Eq. (10) can also be used to derive a simplified expression for the output of an ideal coaxial receiver, which is given by the average pressure over a circular surface S_b with radius b, centered at $w=0$ and parallel to the piston at a distance z. This is a configuration of interest in ultrasonic measurements of attenuation[33,34] as well as hydrophone measurements of acoustic fields.[35] Acoustic reciprocity allows the spatially averaged pressure to be obtained in a similar manner for the cases $b \leqslant a$ and $b > a$. The results can compactly be written as

$$\begin{aligned}\bar{p}_b(z) &= \frac{1}{\pi b^2}\int p(\mathbf{r})\,dS_b \\ &= \frac{\alpha_1^2}{2b^2}\sum_{n=0}^{\infty}(-1)^n\left(\frac{k\alpha_1}{2}\right)^{2n} \\ &\quad\times\frac{(4n+1)\Gamma\left(n+\frac{1}{2}\right)}{\Gamma(n+2)\Gamma\left(2n+\frac{3}{2}\right)}f_{2n}(kz,k\sqrt{z^2+\alpha_2^2}) \\ &\quad\times{}_1F_2\left[n+1;n+2,2n+\frac{3}{2};-\left(\frac{k\alpha_1}{2}\right)^2\right],\end{aligned} \tag{15}$$

where $\alpha_1=b$, $\alpha_2=a$ if $b \leqslant a$, and $\alpha_1=a$, $\alpha_2=b$ if $b>a$. Due to acoustic reciprocity, interchange of source and receiver causes the spatially-averaged pressure to vary only by a multiplicative factor due to the change in relative source and receiver area.[34,35]

C. Recurrence relations for numerical evaluation

Because gamma functions of large order can take on exceedingly large values (e.g., $\Gamma(171) \approx 7.3\times10^{306}$ is the largest integer-order gamma function that can be computed as a double-precision real variable), it is helpful to define recurrence relations for the coefficients in the expansions of Eqs. (8) and (10). Using the recurrence and duplication formulas for the gamma function,[36] the outer expansion of Eq. (8), valid for $r \geqslant a$, is written as

$$\begin{aligned}p(\mathbf{r}) &= \sum_{n=0}^{\infty}A_n{}_1F_2\left[n+1;n+2,2n+\frac{3}{2};-\left(\frac{ka}{2}\right)^2\right] \\ &\quad\times P_{2n}(\cos\theta)h_{2n}^{(1)}(kr), \\ A_0 &= \frac{(ka)^2}{2}, \\ A_n &= -\frac{2n-1}{32n^3-26n+6}(ka)^2A_{n-1}, \quad n>0,\end{aligned} \tag{16}$$

while the paraxial expansion of Eq. (8), valid for $w \geqslant \sqrt{z^2+a^2}$, is written as

$$\begin{aligned}p(\mathbf{r}) &= \sum_{n=0}^{\infty}B_nf_{2n}(kz,kr_a)j_{2n}(kw), \\ B_0 &= 1, \\ B_n &= -\frac{8n^2-2n-1}{8n^2-6n}B_{n-1}, \quad n>0,\end{aligned} \tag{17}$$

with $f_{2n}(kz,kr_a)$ defined by the recurrence relation of Eq. (11).

Similarly, the expansion of Eq. (15) for the pressure averaged over a coaxial circular surface of radius b can be written

$$\begin{aligned}\bar{p}_b(z) &= \sum_{n=0}^{\infty}C_nf_{2n}(kz,k\sqrt{z^2+\alpha_2^2}) \\ &\quad\times{}_1F_2\left[n+1;n+2,2n+\frac{3}{2};-\left(\frac{k\alpha_1}{2}\right)^2\right], \\ C_0 &= \left(\frac{\alpha_1}{b}\right)^2, \\ C_n &= -\frac{2n-1}{32n^3-26n+6}(k\alpha_1)^2C_{n-1}, \quad n>0,\end{aligned} \tag{18}$$

where $\alpha_1=b$, $\alpha_2=a$ if $b \leqslant a$, and $\alpha_1=a$, $\alpha_2=b$ if $b>a$.

III. COMPUTATIONS

Example computations were performed by directly applying the outer series expansion of Eq. (16), the paraxial series expansion of Eq. (17), and the expansion of Eq. (18) for computations of averaged pressure over a circular aperture. In each case, series were truncated after the convergence criterion

$$\frac{|p_n - p_{n-1}|}{|p_{n-1}|} < \epsilon \tag{19}$$

was met for two successive terms, where p_n is the pressure estimate obtained by truncation of an exact series expansion after the nth term. Given this convergence criterion, a

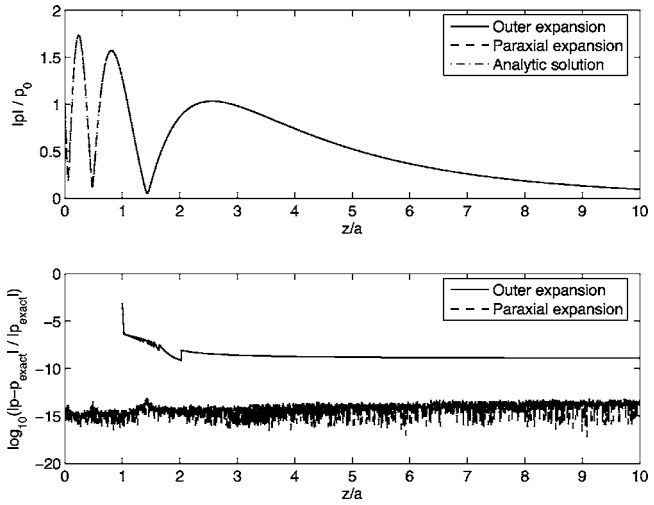

FIG. 2. Computed pressure amplitudes and base-10 logarithm of relative error for paraxial and outer series expansions of the on-axis field of a baffled piston in a lossy medium, computed for $ka=20+0.1i$.

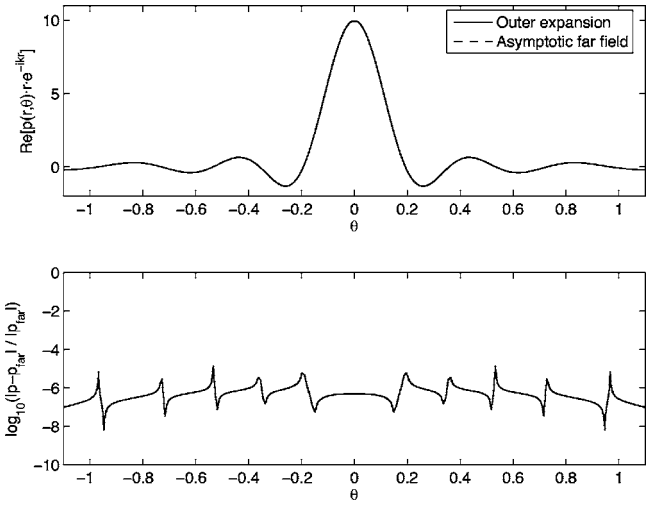

FIG. 3. Computed far-field pattern and base-10 logarithm of error relative to the asymptotic far-field solution for the outer series expansion, computed for $ka=20$, $kz=20\times10^7$.

minimum of three terms is required to compute the piston field at any point. The small parameter ϵ was taken in these computations to be 10^{-6}. If a series computation diverged or caused a floating-point overflow before meeting the convergence criterion, as can occur near the boundaries of convergence for each series type, the sum was taken to be the value obtained by truncating the series at the term of minimum error ϵ.

Results from the exact series expansions derived above can be compared with known analytic solutions for special cases of the piston field. For the on-axis case $w=0$, the paraxial series expansion given by Eq. (10) is mathematically equivalent to the analytic solution of Eq. (12). In Fig. 2, the exact on-axis field for $ka=20+0.1i$ is plotted against the expansions of Eqs. (8) and (10), where the former solution is only valid for $z\geqslant a$. Also shown is the logarithmically scaled relative error $\log_{10}(|p-p_{\text{exact}}|/|p_{\text{exact}}|)$, where p_{exact} is the analytic on-axis solution of Eq. (12). The corresponding plot of error relative to the analytic solution shows that the outer expansion of Eqs. (8) has a numerical error comparable to the truncation error expected for $\epsilon=10^{-6}$, except for the region $z\approx a$. The paraxial expansion of Eq. (10) shows error comparable to the precision limit for double-precision numerical computations.

The solutions can also be compared to the asymptotic far field for the piston radiator, given by

$$p(r,\theta)\rightarrow -ika^2\frac{J_1(ka\sin\theta)}{ka\sin\theta}\frac{e^{ikr}}{r}, \tag{20}$$

where J_1 is the Bessel function of order 1. Figure 3 shows plots of the far-field pattern $p(r,\theta)\cdot re^{-ikr}$ for the asymptotic $(r\rightarrow\infty)$ solution and the present series solutions, computed for a piston with normalized radius $ka=20$, a normalized axial distance of $kz=20\times10^7$, and azimuthal distances of $w<2z$, corresponding to $|\theta|<1.11$ radians or an angular span of 127°. The second panel of the plot shows the logarithmically scaled relative error $\log_{10}(|p-p_{\text{far}}|/|p_{\text{far}}|)$, where p_{far} is the asymptotic far-field solution of Eq. (20). Agreement is good, with error exceeding the series truncation precision only near nulls of the asymptotic far-field pattern.

Convergence of the outer and paraxial series expansions is illustrated in Fig. 4. Here, the number of terms required to meet the convergence criteria described above are plotted as a function of position for a piston with normalized radius $ka=50$. The outer expansion from Eqs. (8) and (16) converges uniformly outside the vicinity $r\approx a$, requiring 35 to 38 terms for most of the field. The paraxial expansion from Eqs. (10) and (17) converges immediately on-axis, with the number of required terms increasing approximately linearly $(N\sim kw)$ as the azimuthal distance w approaches $\sqrt{z^2+a^2}$. For the case illustrated here, convergence occurs in less than 38 terms throughout the cylinder $w\leqslant a$, except for the vicinity where $z\approx0$ and $w\approx a$. Although the number of terms required for convergence depends on ka, the spatial regions of convergence for each expansion are determined only by the piston geometry, as seen from the conditions for validity of Eq. (6).

The two expansions derived above have overlapping regions of validity that enable accurate computation of the radiated pressure field for the entire half-plane $z\geqslant0$. An effective use of these series employs Eqs. (8) or (16) for the region $w\geqslant a$ and Eqs. (10) or (17) for the region $w<a$. The number of terms required for convergence using this combination of series is illustrated in Fig. 4(c). The region of validity for each solution results in rapid convergence everywhere (number of terms $\sim ka$) except for points near the piston boundary, where $z\approx0$ and $w\approx a$.

An example simulation shows the application of these methods to computation of fields induced by high-frequency sources in lossless and absorbing media. This computation employed the outer expansion of Eq. (16) for the region $w\geqslant a$ and the paraxial expansion of Eq. (17) for the region $w<a$. The parameters employed correspond to a transducer of frequency 4 MHz and diameter 6.1 cm radiating into a tissue-like fluid medium with sound speed 1.54 mm/μs. Figure 5 shows pressure amplitudes for the lossless case, with a normalized wave number $ka=500$, and for a case with ab-

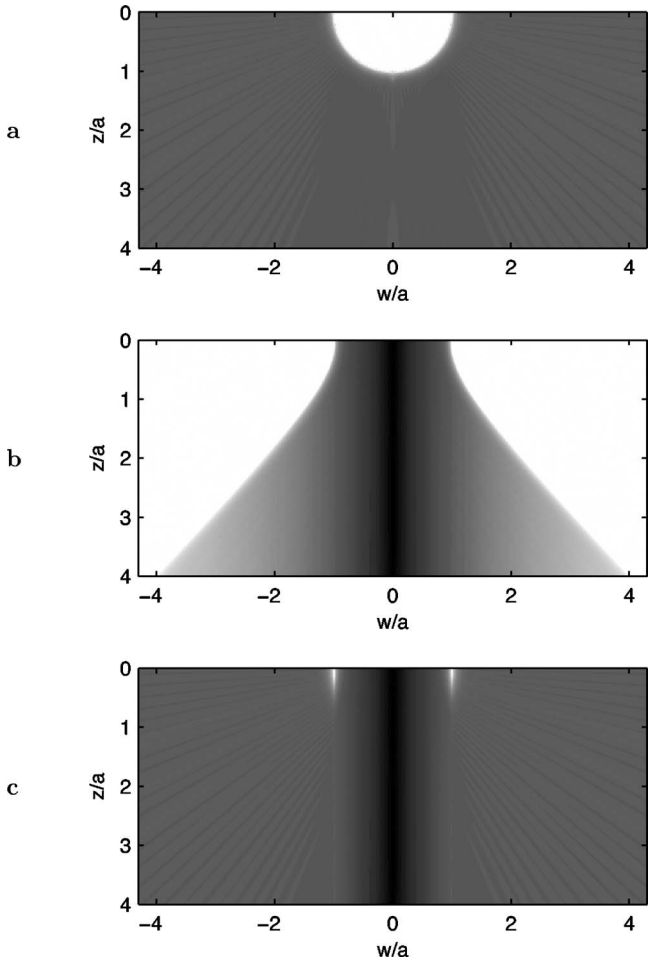

FIG. 4. Number of terms required for convergence, $ka=50$, $\epsilon=10^{-6}$. The number of required terms is shown using a linear gray scale where black represents three terms (the minimum possible for the convergence criteria employed) and white represents 200 terms. To show detail, points requiring more than 200 terms are plotted with a value of 200. (a) Outer expansion. (b) Paraxial expansion. (c) Combined solution, requiring <40 terms in most of the half-space. The solid white regions in panels (a) and (b) represent the spatial regions where the respective expansions do not converge.

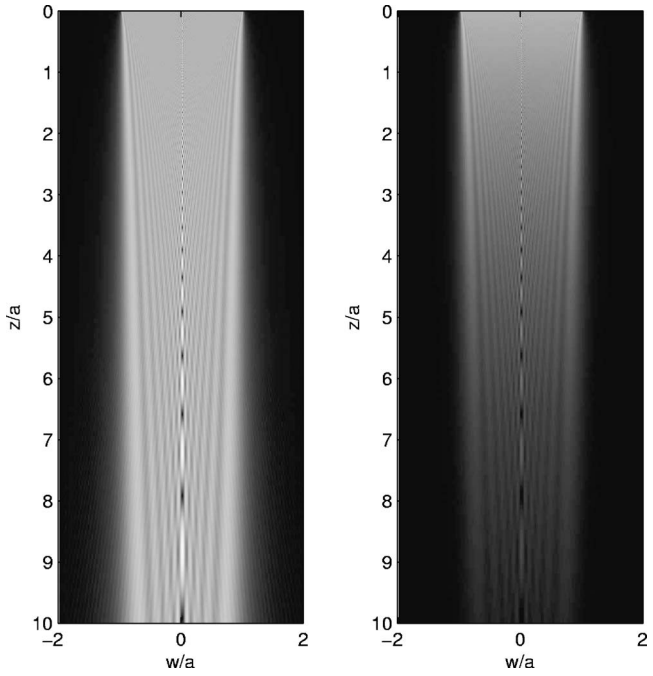

FIG. 5. Pressure amplitude computed using simplified series expansions. Left: field in a lossless medium, $ka=500$. Right: field in an absorbing medium, $ka=500+0.2303i$. Both fields are shown using a linear gray scale in which black represents $|p|=0$ and white represents $|p|=2p_0$.

sorption of 2 dB per piston radius, or 0.16 dB/(cm MHz), corresponding to a normalized complex wave number $ka=500+0.2303i$.

The accuracy and computational efficiency of the exact series expansion approach can be compared with numerical integration using the impulse response method. For the straightforward implementation of the impulse response method employed here, the single-frequency field was obtained here as a single Fourier component of the analytic piston impulse response[9] The Fourier integral defined in Ref. 9 was evaluated analytically for the constant portion of the impulse response, and using midpoint integration for the duration over which the impulse response is not constant. The number of summation points used for the numerical integration was adjusted so that the time step employed was an integer fraction of the time span integrated.

The impulse response method was used to compute the lossless field of a piston with $ka=500$ described above and plotted in Fig. 5. For accuracy comparable to the series method, a sampling rate of about 1000 points per period, or 4 GHz for the present example, is required for the impulse response method. This fine sampling is consistent with previous findings that gigahertz (GHz)-range sampling rates are required for accurate impulse-response computations of megahertz (MHz)-range ultrasound fields.[37] To compute one field point, the impulse response method as implemented here thus required summation of up to 1.59×10^5 terms for each field point. This may be compared to the $\sim$300 summation terms required for the series solution with comparable accuracy in this case. Also notable is that the impulse response must be recomputed for each spatial position, while the series solutions of Eqs. (16) and (17) contain coefficients that need only to be evaluated once for multiple spatial positions. The result is that the impulse-response method required 1.8×10^{-2} CPU s per field point for the computation shown, while the series expansion method required 1.6×10^{-4} CPU s per field point. Thus, for the implementations employed here, the series method can improve computational speed by two orders of magnitude compared to numerical integration. Both computations were implemented here in GNU Fortran 77 (g77), running under Linux on an AMD Athlon 64 3000+ processor with clock speed 1.8 GHz.

Use of the series expansion method to model a pitch-catch measurement is illustrated in Fig. 6. In the modeled configuration, the acoustic pressure radiated by a baffled piston is detected by an idealized coaxial receiver that averages the free-field pressure over a circle of radius a. The averaged pressure was computed using Eqs. (18) for normalized wave numbers $ka=1$, 4, 10, and 100 and axial distances $0<z/a<10$. The results show the expected axial variations in the measured pressure due to near-field diffraction effects, as well as amplitude changes due to beam spreading. The accuracy of these results can be gauged by numerical com-

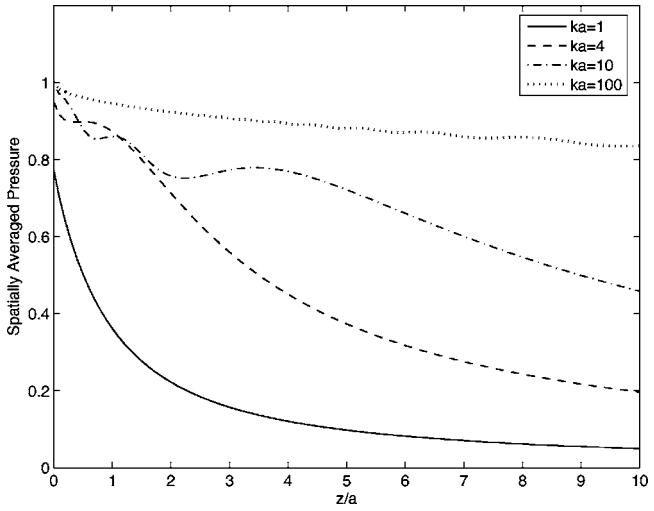

FIG. 6. Acoustic pressure field of a baffled piston averaged over a coaxial circle of equal radius, plotted as a function of normalized axial distance z/a for four values of the normalized wave number ka.

parisons with the exact solution for $a=b$, $z=0$ given by Rayleigh[1,2] and with the numerical integration approach from Ref. 34 for arbitrary a, b, and z. The series method from Eqs. (18) is thus found to provide acceptable accuracy (relative error magnitude $\sim 10^{-4}-10^{-5}$) for $z=0$ and high accuracy (relative error magnitude $<10^{-6}$, limited by the series truncation error) for z greater than about $0.1a$.

IV. DISCUSSION

The work presented here provides accurate solutions for the fields of piston radiators, with favorable analytic and computational simplicity as well as convergence properties compared to previous exact solutions. The outer and paraxial series expansions presented here can be regarded as special cases of those given in Refs. 26 and 27, but consideration of these special cases has resulted in simpler analytic forms for the expansions. Compared to the general expansions given in Refs. 26 and 27, those presented here have one-half the number of terms, take simpler forms including closed-form coefficients for the outer expansion of Eq. (8), and do not require choice of an arbitrary origin position.

The series methods presented here can be considered a complementary alternative to numerical integration approaches. Methods for computing exact piston fields by numerical integration include transformations of the Rayleigh integral into single line integrals[3–6] as well as approaches to integration of the space- and time-dependent piston impulse response.[7–9] Recent progress has been made in efficient numerical computation of such integrals.[10–12] Several approaches are reviewed in Ref. 12, where application of a grid-sectoring method to a modified impulse-response integral is shown to significantly improve computational efficiency for single-frequency computations of the piston nearfield. Compared to the present series approaches, numerical integration approaches based on the piston impulse response may incur greater computational difficulties in the acoustic far field,[10,12] but may provide more accurate results for points near the velocity discontinuity at the piston boundary, where $z\approx 0$ and $w\approx a$.

The series solutions presented here are expected to be useful for computations of single-frequency piston fields at multiple spatial positions. This is the configuration of interest, for example, in ultrasonic heating of tissue, where the acoustic heat deposition in an absorbing medium needs to be known with high spatial resolution.[13] In highly absorbing media, such as soft tissue at sufficiently high ultrasonic frequencies, acoustic absorption may substantially affect diffraction of ultrasound beams. Thus, the series methods presented here, which treat attenuation effects exactly by incorporation of a complex wave number, may have advantages over other approaches that treat attenuation approximately.[13,17,38]

Another application for the series solutions presented here is benchmarking of numerical methods for radiation from arbitrary sources, as has been previously done using numerical integration methods.[16,39] The easily-characterized accuracy of the series solutions allows numerical evaluation of piston radiator fields with accuracy limited only by the floating-point resolution employed in the computations. Thus, this method is expected to be useful for computing reference solutions in both lossless and absorbing media. Using Fourier synthesis of piston fields computed for multiple frequencies, time-domain reference solutions can also be computed. However, the series methods considered here are not expected to be as efficient as time-domain integration methods for computation of transient radiation.

The capability of the series solutions for exact nearfield computations of spatially-averaged piston fields in absorbing media should also be useful for measurements of attenuation in transmission mode.[33,34] In highly absorbing media, the presence of large attenuation may measurably affect the spatial distribution of acoustic pressure in the near field. For this reason, rigorously accounting for the effects of absorption may provide increased accuracy in diffraction correction for attenuation measurements.

[1] J. W. S. Rayleigh, *The Theory of Sound*, Vol. 2, 1896 (reprinted by Dover, New York, 1945), Secs. 278, 302.
[2] A. D. Pierce, *Acoustics: An Introduction to its Physical Principles and Applications*, 2nd ed. (Acoustical Society of America, Woodbury, NY, 1989), pp. 213–245.
[3] L. V. King, "On the acoustic radiation field of the piezo-electric oscillator and the effect of viscosity on transmission," Can. J. Res. **11**, 135–155 (1934).
[4] A. Schoch, "Betrachtungen über das Schallfeld einer Kolbenmembran," Akust. Z. **6**, 318–326 (1941).
[5] S. Ohtsuki, "Ring function method for calculating nearfield of sound source," J. Bronchol. **123**, 23–31 (1974).
[6] G.-P. J. Too, "New phenomena on King integral with dissipation," J. Acoust. Soc. Am. **101**, 119–124 (1997).
[7] F. Oberhettinger, "On transient solutions of the baffled piston Problem," J. Res. Natl. Bur. Stand., Sect. B **65B**, 1–6 (1961).
[8] P. R. Stepanishen, "The time-dependent force and radiation impedance on a piston in a rigid infinite planar baffle," J. Acoust. Soc. Am. **49**, 841–849 (1970).
[9] J. C. Lockwood and J. G. Willette, "High-speed method for computing the exact solution for the pressure variations in the nearfield of a baffled piston," J. Acoust. Soc. Am. **53**, 735–741 (1973).
[10] J. D'hooge, J. Nuyts, B. Bijnens, B. De Man, P. Suetens, J. Thoen, M.-C. Herregods, and F. Van de Werf, "The calculation of the transient near and

far field of a baffled piston using low sampling frequencies," J. Acoust. Soc. Am. **102**, 78–86 (1997).
[11]U. P. Svensson, K. Sakagami, and M. Morimoto, "Line integral model of transient radiation from planar pistons in baffles," Acust. Acta Acust. **87**, 307–315 (2001).
[12]R. J. McGough, T. V. Samulski, and J. F. Kelly, "An efficient grid sectoring method for calculations of the near-field pressure generated by a circular piston," J. Acoust. Soc. Am. **115**, 1942–1954 (2004).
[13]W. L. Nyborg and R. B. Steele, "Nearfield of a piston source of ultrasound in an absorbing medium," J. Acoust. Soc. Am. **78**, 1882–1891 (1985).
[14]H. O. Berktay and M. J. Lancaster, "An analytical expression for the near field of a circular piston radiator," J. Sound Vib. **137**, 319–325 (1990).
[15]A. Freedman, "Acoustic field of a pulsed circular piston," J. Sound Vib. **170**, 495–519 (1994).
[16]T. Xue, W. Lord, and S. Udpa, "Numerical analysis of the radiated fields of circular pistons and time-delay spherically focused arrays," IEEE Trans. Ultrason. Ferroelectr. Freq. Control **43**, 78–87 (1996).
[17]A. Goldstein, "Steady state unfocused circular aperture beam patterns in nonattenuating and attenuating fluids," J. Acoust. Soc. Am. **115**, 99–110 (2004).
[18]H. Backhaus, "Das Schallfeld der kreisförmigen Kolbenmembran," Ann. Phys. **5**, 1–35 (1930).
[19]H. Stenzel, "Über die Berechnung des Schallfeldes einer kreisförmigen Kolbenmembran," Elektr. Nachr. Tech. **12**, 16–30 (1935).
[20]R. C. Wittmann and A. D. Yaghjian, "Spherical-wave expansions of piston-radiator fields," J. Acoust. Soc. Am. **90**, 1647–1655 (1991).
[21]R. D. Spence, "The diffraction of sound by circular disks and apertures," J. Acoust. Soc. Am. **20**, 380–386 (1948).
[22]A. H. Carter and A. O. Williams, Jr., "A new expansion for the velocity potential of a piston source," J. Acoust. Soc. Am. **23**, 179–184 (1951).
[23]A. H. Carter and A. O. Williams, Jr., "A new expansion for the velocity potential of a piston source," [Erratum], J. Acoust. Soc. Am. **24**, 230 (1952).
[24]H. Elrod, "A more rapidly-convergent expansion for the velocity potential of a piston source," J. Acoust. Soc. Am. **24**, 325–326 (1952).
[25]R. New, "A limiting form for the nearfield of the baffled piston," J. Acoust. Soc. Am. **70**, 1518–1526 (1981).
[26]T. Hasegawa, N. Inoue, and K. Matsuzawa, "A new rigorous expansion for the velocity potential of a circular piston source," J. Acoust. Soc. Am. **74**, 1044–1047 (1983).
[27]T. Hasegawa, N. Inoue, and K. Matsuzawa, "Fresnel diffraction: Some extensions of the theory," J. Acoust. Soc. Am. **75**, 1048–1051 (1984).
[28]G. N. Watson, *A Treatise on the Theory of Bessel Functions* (Cambridge University Press, Cambridge, 1922), p. 366.
[29]A. P. Prudnikov, Yu. A. Brychkov, and O. I. Marichev, *Integrals and Series, Volume 2: Special Functions* (Gordon and Breach Science, New York, 1986), p. 37.
[30]A. P. Prudnikov, Yu. A. Brychkov, and O. I. Marichev, *Integrals and Series, Volume 3: More Special Functions* (Gordon and Breach Science, New York, 1990), pp. 608–609.
[31]W. F. Perger, A. Bhalla, and M. Nardin, "A numerical evaluator for the generalized hypergeometric series," Comput. Phys. Commun. **77**, 249–254 (1993).
[32]S. Wolfram, *The Mathematica Book*, 4th ed. (Cambridge University Press, New York, 1999), pp. 772, 1158.
[33]H. Seki, A. Granato, and R. Truell, "Diffraction effects in the ultrasonic field of a piston source and their importance in the accurate measurement of attenuation," J. Acoust. Soc. Am. **28**, 230–238 (1956).
[34]K. Beissner, "Exact integral expression for the diffraction loss of a circular piston source," Acustica **49**, 212–217 (1981).
[35]A. Goldstein, D. R. Gandhi, and W. D. O'Brien, "Diffraction effects in hydrophone measurements," IEEE Trans. Ultrason. Ferroelectr. Freq. Control **45**, 972–979 (1998).
[36]P. J. Davis, "Gamma function and related functions," in *Handbook of Mathematical Functions*, edited by M. Abramowitz and I. A. Stegun (National Bureau of Standards, reprinted by Dover, New York, 1974), Chap. 6.
[37]J. A. Jensen, "A model for the propagation and scattering of ultrasound in tissue," J. Acoust. Soc. Am. **89**, 182–191 (1991).
[38]J. A. Jensen, D. Gandhi, and W. D. O'Brien, "Ultrasound fields in an attenuating medium," 1993 IEEE Ultrasonics Symposium Proceedings, pp. 943–946.
[39]D. Ding and Y. Zhang, "Notes on the Gaussian beam expansion," J. Acoust. Soc. Am. **116**, 1401–1405 (2004).